



Nanostructured TiO₂ Thin Films Deposited by Spray Ultrasonic Nebulizer Technique



Mohammed K. Khalaf^{1*}, Firdous Sh. Ahmed², Ruaa M. Saleh Al-alWany³

¹Materials Research Directorate, Ministry of Science and Technology, Baghdad, Iraq.

²Division of Basic Science, College of Agriculture Engineering Science, University of Baghdad, Iraq.

³Dept. of Chemistry, College Of Education for Pure Science, University of Anbar, Anbar, Iraq

THIS work details the growth of nanostructured TiO₂ thin films on a glass substrates using the ultrasonic nebulizer technique, deposited at 300-600 °C (substrate). The influence of the deposition temperature is linked to the physic-chemical properties of the TiO₂ thin films. XRD- results confirmed that the nanostructures tetragonal are polycrystalline, the grain size(s) increases alongside the substrates temperature, and the deposited film is the anatase phase at 400 °C. The surface morphology of the deposited film were imaged using the (AFM) technique, and it was confirmed that the films are of excellent crystallinity and are homogeneously dispersed. It was also confirmed that the Root Mean Square (RMS) of the thin films' surface roughness is dictated by the substrate's temperature, which was further confirmed using the SEM technique. The substrate temperature is inversely proportional to the optical energy gap values. The increase in optical gap with increasing substrate temperature can be due to improvement in the films crystallinity .At higher temperatures promote a high mobility of ad-atoms; it allows a better atomic arrangement, which promotes the formation of a crystalline structure.

Keywords: TiO₂ films, spray technique, Substrate temperature, Morphological properties.

Introduction

The ultrasonic nebulizer is a simple and inexpensive technique that can produce a large area of well adhered and uniform films. The approach's advantage is the fact that it generates minuscule droplets and project them intricately on a substrate at minimal "bounce back" influence from a targeted surface [1]. This makes it possible for synthesis of superior transfer coefficients relative to conventional coating technologies [2]. Sono-Tek Corporation has developed and patented commercial ultrasonic atomization systems for challenging applications in multiple industries [3]. This article describes Sono-Tek's most recent technology releases for the dispensation and coating of nanoparticles [4-5]. Ultrasonic atomization is a proven spray coating technology that results in unparalleled functional and economic performance, especially in the case of applications where

expensive chemical solutions and suspensions need to be accurately and uniformly deposited onto designated substrates. The ultrasonic nebulizer manipulates electrical signals and turns them into high frequency ultrasonic waves. The transducer resonates at the frequency of the ultrasonic waves it is exposed to (piezo electric effect), which are then transmitted to the surface of the solution to form aerosol ultrasonic nebulizers include [6], standard nebulizers, where the material comes into direct contact with the piezo-electric transducer, causing the material's temperature to increase from the heat the transducer is exposed to and ultrasonic nebulizers, where the water interface utilize the water present between the piezo-electric transducer and a separate reservoir. The omnipresent water keeps the temperature of the material low and keeps it away from the transducer [7]. TiO₂ thin films were deposited onto a glass substrate using the Spray Ultrasonic Technique,

*Corresponding author e-mail: mohammedkhkh@yahoo.com

Received 25/9/2019; Accepted 12/1/2020

DOI: 10.21608/ejchem.2019.17350.2064

©2020 National Information and Documentation Center (NIDOC)

and the effect of substrate's temperature on the physico-chemical properties of the thin films were subsequently determined.

Experimental

The titanium dioxide (purity 99.9%, Sigma-Aldrich, USA) thin film was prepared using the ultrasonic nebulizer technique. The ultrasonic nebulizer was linked to quartz and cylinder tubes to facilitate the placement chemical solution. The parametric setting of the experimental are detailed in Figure (1, 2) and Table (1). Glass substrates with dimensions of 10 mm × 10 mm were cleaned using acetone and methanol submerged in an ultrasonicator, first, then in distilled water. The glass substrates were then dried in an oven. To create a perfect solution, 1.5g of (Ti₂O) nanopowder was dissolved in 500 ml of distilled water, and then stirred (MSH-300, magnetic Stirrer with hot plate) for 5mins until the solution is thoroughly mixed. The concentration of the solution is critical due to the fact that that it dictates the success/failure of the deposition of TiO₂ thin films. The glass

substrates were placed in the middle of the hot plate. One side of the quartz tube was linked to an ultrasonic nebulizer, which was done to help the hot plate realize its designated temperature. Upon realizing its designated temperature, the ultrasonic nebulizer was turned on. It (Model NE-U17, Omron Matsusaka Co. Ltd., Japan), comes equipped with a 1.67MHz transducer, and it is used to atomizes chemical solution into fine droplets (streams). Vibrating transducer turns the precursor solution into concentrated aerosol. The nebulized spray goes up into the column, then deposited onto a hot substrate. The formed film was then further heat treated to increase the quality of the deposited films.

It can be seen that when the spray solution is high concentration, cracks will form on the deposited films and the surface morphology becomes quite rough. Substrates temperature was controlled using a thermocouple, and was adjusted accordingly during the deposition process. The hotplate was switched off after the films were deposited and allowed to air cool [7-9].

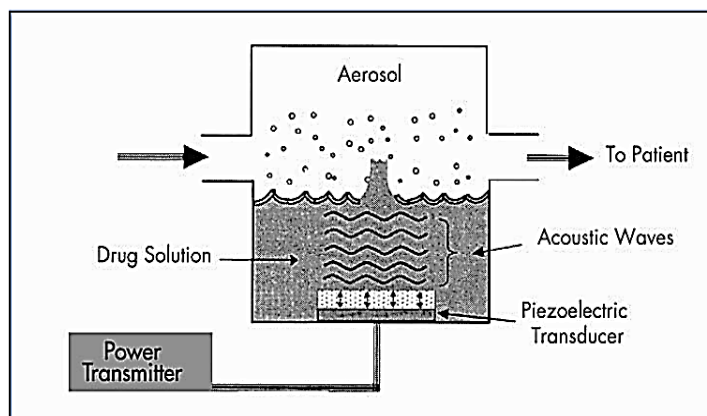


Fig. 1. Component of an ultrasonic nebulizer

TABLE 1. Technical parameters of ultrasonic nebulizer

	Voltage	AC220+10%
Ultrasonic frequency		1.7MHz+10%
Max capacity of medicine for big cup		350 ml
Max medication capacity for small cup		150ml
Max nebulizing rate		3>ml/min
Consumption power		50< W
Continues working time		> 4h

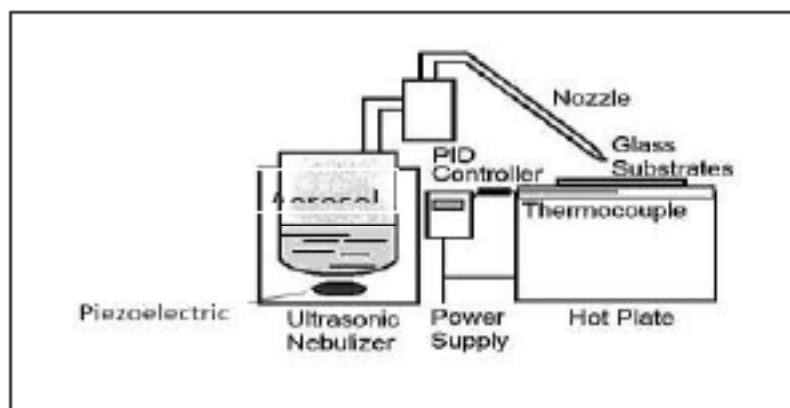


Fig. (2). Schematic diagram of ultrasonic nebulizer setup

Results and Discussions

Structural Properties

XRD Analysis

The XRD diffractogram of the as-grown TiO₂ films sputtered at multiple temperatures onto glass substrates are shown in Fig (3). The increasing deposition temperature converted the fully amorphous state of the deposited film into a partially anatase crystalline phase films deposited at 300 °C and 400 °C exhibited no diffraction peaks, which means that the films are amorphous, or that the crystallites are too small to be detected by the X-rays, as per [10]. At deposition temperatures of 500 °C and 600 °C, the detected peaks are that of the polycrystalline anatase (A) phase only, with intensities of (101), (004) and (105) thin films in the case of the former, and (101), (004) and (200) in the case of latter as per Figs. (3), which are in agreement with the values in the (ASTM) card. There are no typical rutile peaks present at this (relatively) high annealing temperature. The average crystallite size of the particle's in the films increased, from its initial size 30.1 nm to 37.2 nm, in tandem with the increasing temperature. The crystallite size (D_{ave}) of the TiO₂ thin film was determined using the Scherrer's equation, and it was confirmed that it is directly proportional to the films' thickness, which can be attributed to the lack of defects. These occurrence are detailed in Table (2). The increased deposition temperature converts the fully amorphous anatase state of the deposited films to a partially crystalline anatase thin film [10]. In comparison with the traditional (pneumatic) technique, the ultrasonic spray pyrolysis technique allows the deposition of both crystalline and amorphous TiO₂ thin films with a high quality, in a fast and reproducible way.

Atomic Force Microscope (AFM) Measurements

AFM scans were conducted within the area measuring, (10 × 10) μm² on the films annealed at 300-600 °C. and it was confirmed that microstructure of the deposited film changes with increasing temperatures. Agglomeration of the nanoparticles were also evident in the AFM scans. The AFM scans also allowed us to determine the average surface roughness and the roughness and mean square values, and the results are detailed in Figure (4) and Table (3). Results shows that, the ultrasonic nebulizer technique allows obtaining optically smooth, uniform and homogeneous layers. The Roughness value of the TiO₂ thin film was determined very low, and this supposition was further supported by the SEM image of the thin film (smooth). It was also surmised that the roughness is directly correlated to the annealing temperature, and increased roughness also resulted in increased grain size. The most likely factor for the dramatic topographic change is the recrystallization in the films, which could be attributed to thermal annealing [10]. The larger grains or hillocks on the surface of the films confirmed the improved crystallinity of the TiO₂ films.

Scanning Electron Microscope (SEM)

Fig. (5) details the SEM micrographs of the TiO₂ thin film deposited on a quartz substrate at designated deposition temperatures (300, 400, 500 and 600 °C). The TiO₂ thin films are seen to be uniform and hole-free, and a wide-sized distribution of particle size. The film deposited at a substrate temperature of 300 °C exhibited needle-type grain growth, and its shape was altered from granular to plate-like when the temperature increased from (400 °C to 600 °C). It was also made evident that the particle size is directly proportional to deposition temperature in this case. The particle

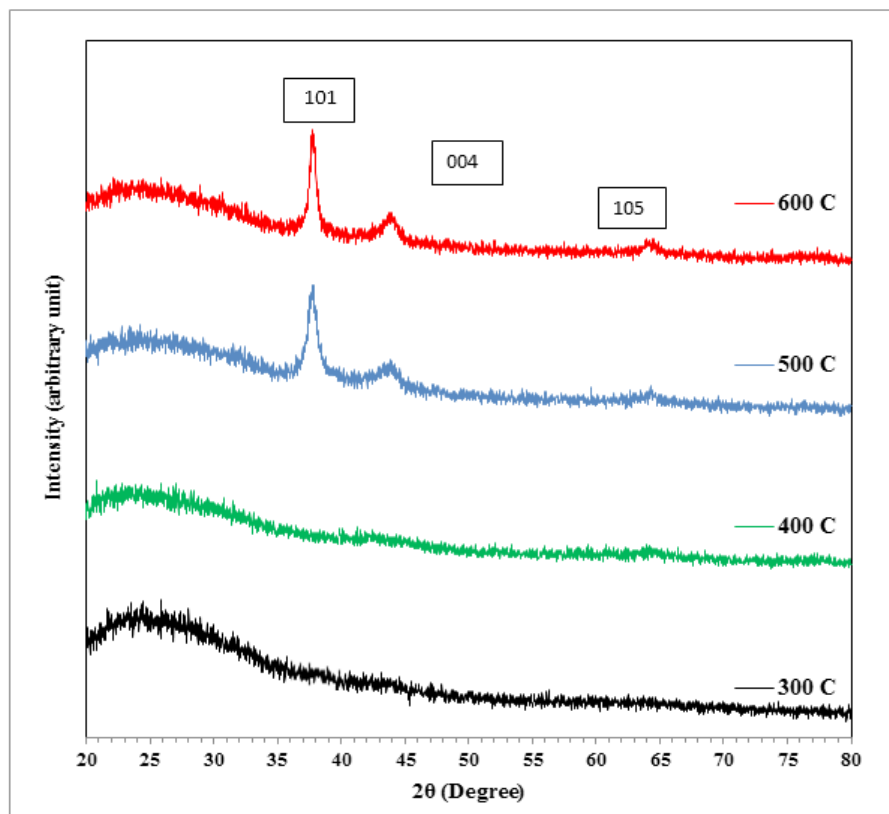


Fig. 3. XRD patterns of TiO₂ thin film for different temperature.

TABLE 2. Some structural properties for TiO₂ thin films.

Material	Temp. °C	hkl	B_{θ}	β	D_{ave} (nm)	Phase	$\delta \times 10^{11} / \text{cm}^2$	$N_o \times 10^{11} / \text{cm}^2$
TiO ₂	500	101	12.66	0.0049	30.107	Anatase	1.103	3.66
		004	18.63	0.0054				
		105	26.69	0.0061				
TiO ₂	600	101	12.66	0.0039	37.249	Anatase	0.719	3.85
		004	18.93	0.0041				
		105	24.01	0.0031				

TABLE 3. Surface roughness and root square measurements for TiO₂ thin films.

Temperature °C	Surface Roughness (nm)	RMS (nm)	Grain Size (nm)
300	1.244	1.842	18.3
400	2.498	3.452	19.24
500	2.568	3.684	20.35
600	2.965	4.012	25.24

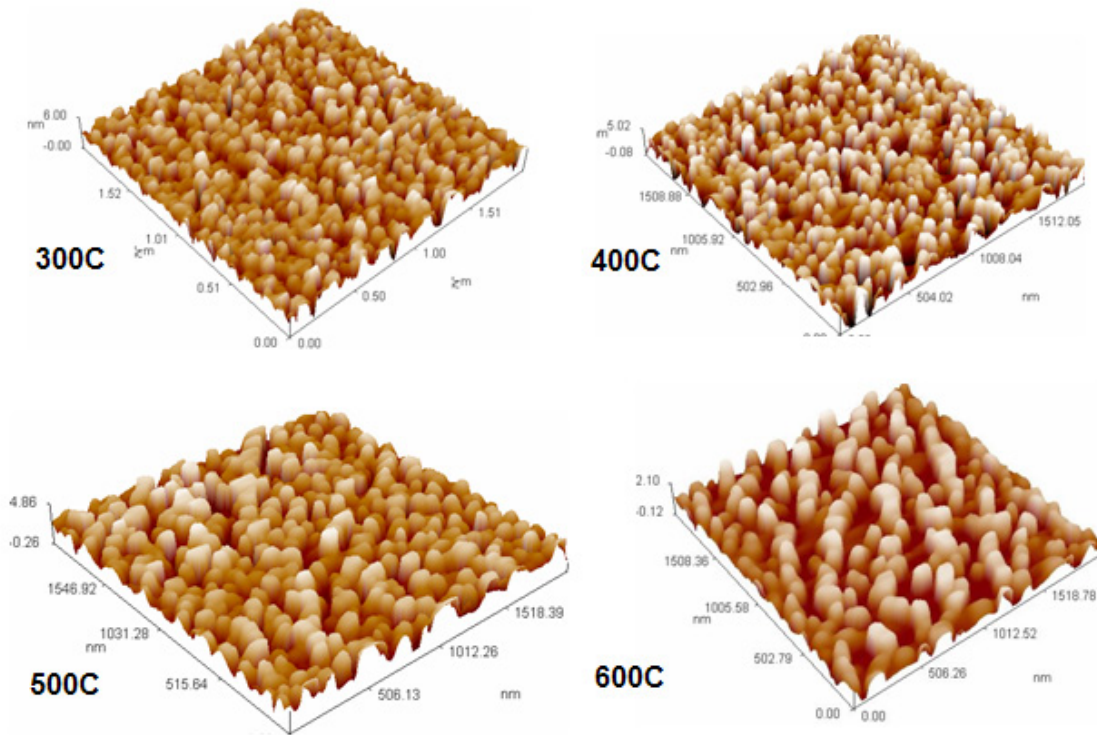


Fig. 4. AFM images for TiO₂ thin films film deposited at different substrate temperature of 300- 600 °C.

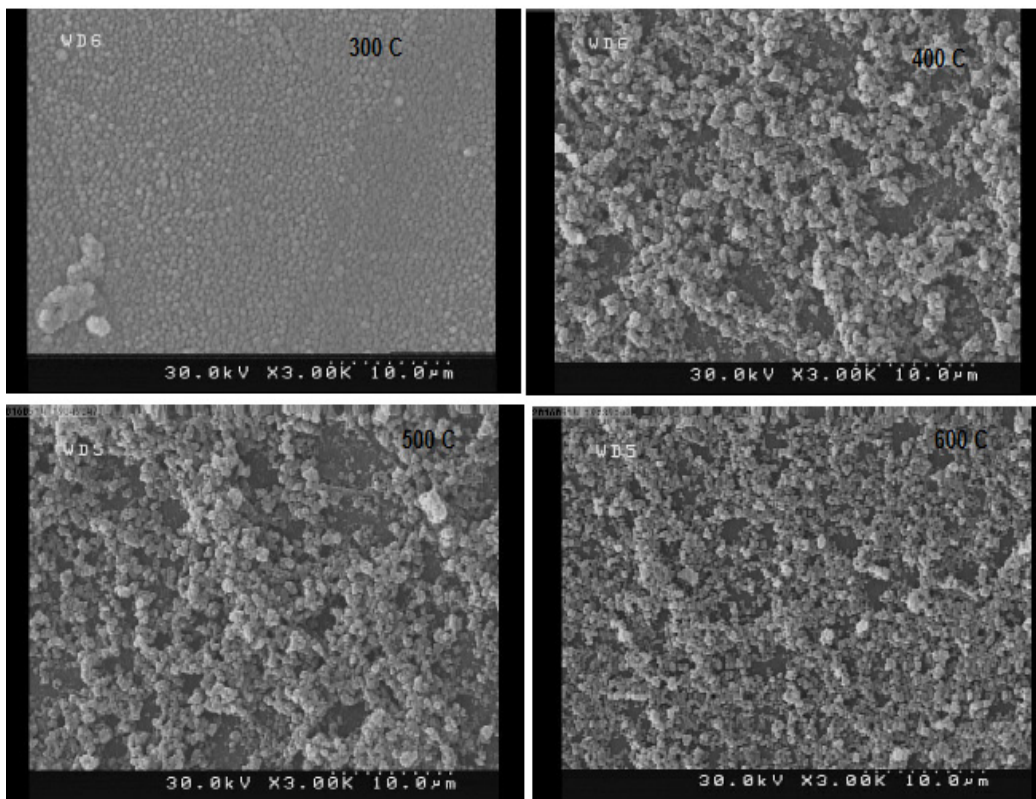


Fig. 5. SEM image of the TiO₂ thin films film deposited at different substrate temperature of 300- 600 °C.

size determined from the SEM micrographs those determined from XRD diffractograms. This could be due to the latter reporting, the average crystallite size, while the former reported the size of the agglomerated particles. The deposited films are made up of nanostructures, and are mostly homogeneous. It was also previously surmised that the average size of the aggregated/ agglomerated particles are dependent on the substrate deposition temperature, and the subsequent annealing temperature of the thin post-deposition. Figure 5 shows SEM micrographs of iron oxide films deposited at 300 and 600 °C; both films show different surface morphology. As it is evidenced in the figure, films deposited at 600 °C are rougher than films deposited at 300°C. This phenomenon is due to the fact that droplets evaporate before they reach the substrate surface, promoting the precipitation of the precursors. Therefore, the kinetic energy of ad-atoms decreases and forms rough surfaces. On the other hand, at the optimum substrate temperature, the pyrolytic reaction takes place at the gas-substrate surface interface; it promotes the synthesis of smoother films similar to those obtained by a - CVD process. For optimal deposition temperatures, the ultrasonic technique allows to produce homogeneous and smoother films that those obtained by a pneumatic spraying.

Optical Properties

The optical transmittance of TiO₂ films on glass prepared by the ultrasonic spray technique (USS) was determined using the UV-Vis spectrophotometer. Transmittance is dependent upon temperatures, as can be seen in Fig (6). The average transmittance of the TiO₂ thin film exceeded 90% in the near-infrared region, which means that the film are applicable as window materials in solar cells. It can also be seen in the

case of all of the deposited films that the optical transmittance is inversely related to substrate temperature, which can be attributed to the increased roughness resulting in increased light scattering.

Absorption

The optical absorbance of pure TiO₂ films prepared by ultrasonic nebulizer technique was also determined using the UV-Vis spectrophotometer. It was subsequently confirmed that the absorbance of the deposited thin films are strongly reliant temperature, as per Fig (7). It was also confirmed that the absorbance of the deposited TiO₂ thin films are strongly correlated to the substrate temperature. Which can be attributed to the increased particle sizes and surface roughness. The absorption edges of the TiO₂ films reported a small red shift when the substrate temperature was increased.

Optical Energy Gap

The energy gap values of the deposited thin films' are in general dependent upon its crystal's structure. Arrangement/and distribution of atoms within crystal lattice are influenced by regularity, and in order to accurately the value of the direct band gap of the thin film, we utilized Tauc's relationship. TiO₂ possess direct/indirect band gaps, whose values change based on parameters processing conditions. The graphs of $(\alpha h\nu)^2$ vs E (eV) in the case of the direct band gap of TiO₂ thin film are detailed in Figure (8). Graphs in the case of the order deposited thin films report similar type of plot. The values of E_g was obtained by extrapolating $(\alpha h\nu)^n = 0$. The E_g ° values for the direct band gap all the thin films are summarized in Table (1). The optical band gap values for both transitions differ from that of the well-known values of 3.2 eV in the case of TiO₂ anatase. The

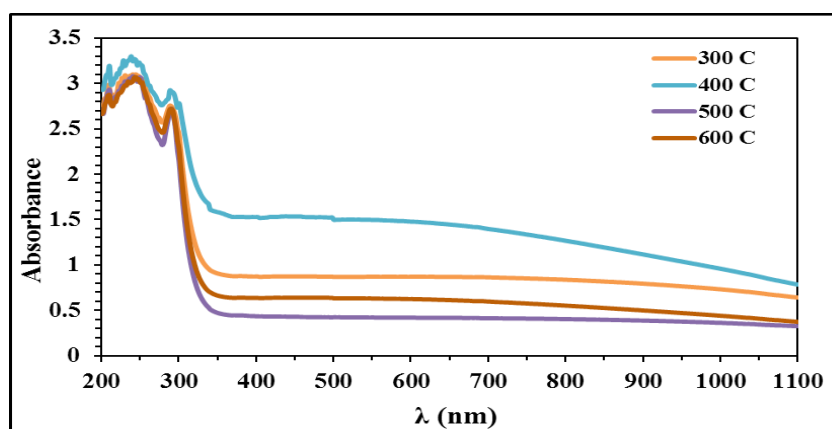


Fig. 6. UV-VIS transmittance spectra of the TiO₂ films film deposited at different substrate temperature of 300- 600 °C.

direct band gap value obtained for the deposited TiO₂ thin film is 3.44 eV, which is in line with values reported [10]. The direct optical transition reported for TiO₂ anatase is detailed in Table (4). The substrate temperature is inversely proportional to the optical energy gap values. This could be due to the increasing substrate temperature decreasing structural defects, which decreases the optical energy gap as per Figure (8).

Absorption coefficient

The absorption coefficient of the pure deposited TiO₂ thin film was determined and Figure (9) details the variation of (α) as a function of photon energy and wavelength. Its value is larger than (10^4 cm^{-1}) all of the deposited films. It can also be seen that the increased absorption coefficient and substrate temperature occur due to

the increased film thickness due to the absorption of light, mostly attributed to the formation stage of anatase and increased grain size. This makes ultrasonic nebulizer deposited thin films excellent candidates for large-scale applications in gas sensors, solar cells, lithium-ion batteries, low emission window, and UV photodetectors [11].

Conclusion

The effect of substrate temperature on the growth of TiO₂ thin film deposited using the spray USS technique were investigated. TiO₂ thin films were deposited onto glass substrates at multiple (deposition) temperature. The optical properties of the deposited thin films were determined. It was confirmed that the surface morphology is greatly affected by substrate temperature, which was evident in the SEM images. The films were

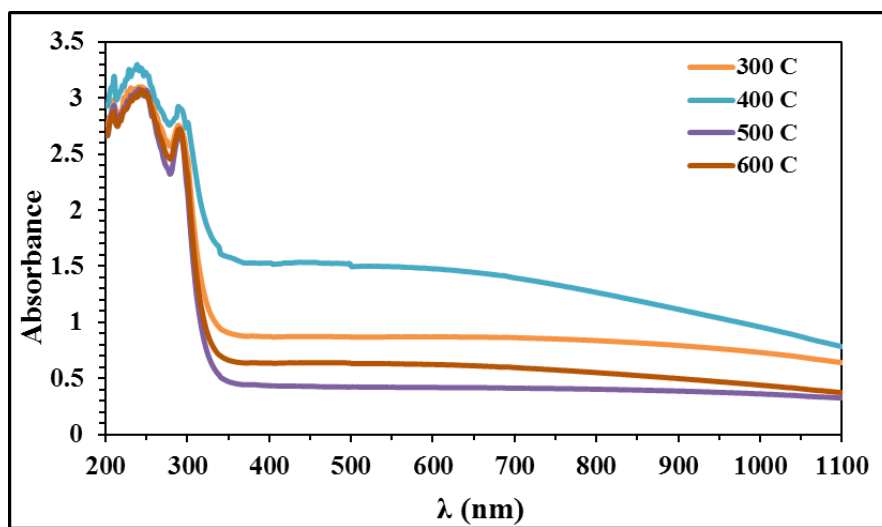


Fig.7. UV-VIS absorption spectra of the TiO₂ films at different substrate temperature

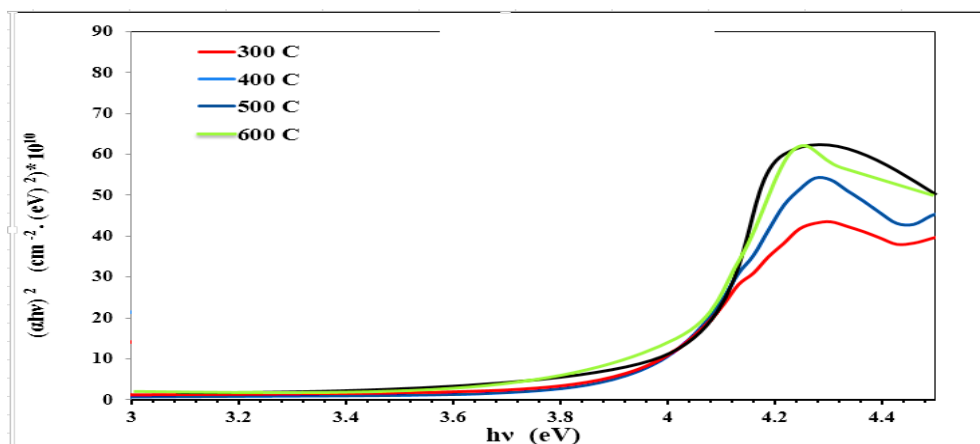


Fig. 8. $(\alpha h\nu)^2$ as a function of photon energy of TiO₂ thin film.

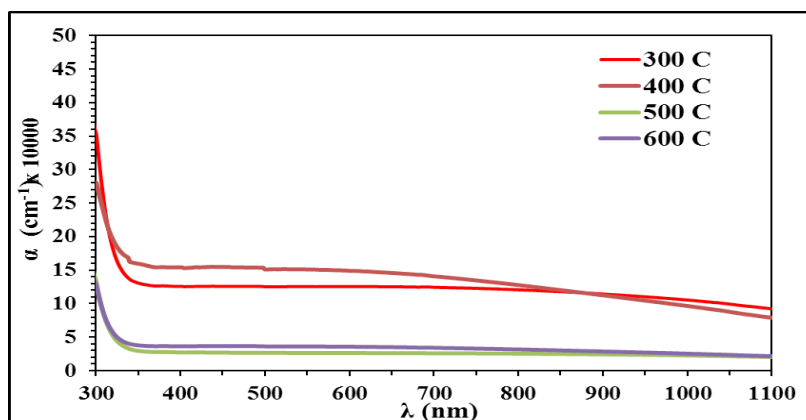


Fig. 9. Absorption coefficient as function of energy photon for TiO_2 .

TABLE 4. Optical band gap and thickness of TiO_2 films of different temperature.

Temperature ($^{\circ}\text{C}$)	Energy gap (eV)	Thickness(nm)
300	3.99	46
400	3.88	66
500	3.85	106
600	3.61	120

determined to be transparent in the visible region. The inverse relationship between optical band gap and substrate temperature was due to the phase transformation to rutile (lower band gap than the anatase phase). It can be concluded that amorphous films present the best optical behavior (higher transmission) for the design of thin film solar filters. The results obtained were satisfactory, and the Spray Ultrasonic Nebulizer system demonstrates advantages such as simplicity, rapidity, high sensitivity, and low cost.

References

- Jian hui Zhang and Wei Li, Synthesis of High-Density Vertically Aligned Carbon Nanotubes Using Ultrasonic Nebulizer. *Materials Sciences and Applications*, **3**, 213-217 (2012).
- Feng Guo dong and Jeanjie, Evaluation of Improved Ultrasonic Nebulizer for Miniature Simultaneous Microwave Plasma Torch Spectrometer. *Science Direct, CHEM. RES. CHINESE U.* **22**(3), 297-301, (2006).
- Mann M. , Zhang Y. , Teo K. B. K. , Wells T., El Gomati M. M. and Milne W. I., Controlling the Growth of Carbon Nanotubes for Electronic Devices, *Microelectronic Engineering*, **87** (5-8), 1491-1493 (2010).
- Jin Q., Zhu C., Brushwyler K. and Hieftje G.M., An efficient and inexpensive ultrasonic nebulizer for atomic spectrometry, *Appl. Spectrosc.* **44**, (1990).
- Jankowski K., Karmasz D., Ramsza A. and Reszke E., Characteristics of nebulizers for microwave induced plasma atomic emission spectrometry. II. Ultrasonic nebulizers, *Spectrochim. Acta Part B* **52**, (1997).
- Carvalho T. C. and McConville J. T. , The function and performance of aqueous aerosol devices for inhalation therapy, *Journal of Pharmacy and Pharmacology*, **68**, 556-578 (2016).
- Matusiewicz H., and Ślachciński M., Analytical evaluation of an integrated ultrasonic nebulizer-hydride generator system for simultaneous determination of hydride and non-hydride forming elements by microwave induced plasma. *Spectrometry, Spectrosc. Lett.* **43**, 474–485 (2010).
- Maehara N., Ueha S. and Mori E., Influence of the vibrating system of a multipinhole plate ultrasonic nebulizer on its performance, *Review of Scientific Instruments*, **57**, 2870 (1986).
- Tarr M.A., Zhu G., Browner R.F., Microflow ultrasonic nebulizer for inductively coupled plasma atomic emission spectrometry, *Anal. Chem.* **65**, 1689–1695 (1993).
- Shiosaki T. , Yamamoto T. , Yagi M. and Kawabata A. *App. Phys. Lett.* **39**, 399 (1981).
- Kacha Deyu G., Muñoz-Rojas D., Rapenne L., Deschanvres J., Klein A., Jiménez C., Bellet D., SnO_2 Films Deposited by Ultrasonic Spray Pyrolysis: Influence of Al Incorporation on the Properties, *Molecules*. **24**(15), 2797 (2019).